



Heriot-Watt University
Research Gateway

Optimisation and analysis of a heat pipe assisted low-energy passive cooling system

Citation for published version:

Chaudhry, HN, Calautit, JK & Hughes, BR 2017, 'Optimisation and analysis of a heat pipe assisted low-energy passive cooling system', *Energy and Buildings*. <https://doi.org/10.1016/j.enbuild.2017.02.002>

Digital Object Identifier (DOI):

[10.1016/j.enbuild.2017.02.002](https://doi.org/10.1016/j.enbuild.2017.02.002)

Link:

[Link to publication record in Heriot-Watt Research Portal](#)

Document Version:

Peer reviewed version

Published In:

Energy and Buildings

Publisher Rights Statement:

© 2017 Elsevier B.V.

General rights

Copyright for the publications made accessible via Heriot-Watt Research Portal is retained by the author(s) and / or other copyright owners and it is a condition of accessing these publications that users recognise and abide by the legal requirements associated with these rights.

Take down policy

Heriot-Watt University has made every reasonable effort to ensure that the content in Heriot-Watt Research Portal complies with UK legislation. If you believe that the public display of this file breaches copyright please contact open.access@hw.ac.uk providing details, and we will remove access to the work immediately and investigate your claim.

Optimisation and analysis of a heat pipe assisted low-energy passive cooling system

*Dr. Hassam Nasarullah Chaudhry*¹

School of Energy, Geoscience, Infrastructure and Society, Heriot-Watt University, PO Box 294
345, Dubai, United Arab Emirates

Contact: +971 (0) 4 435 8775, Email: H.N.Chaudhry@hw.ac.uk

Dr. John Kaiser Calautit

Department of Mechanical Engineering, University of Sheffield, S10 2TN, UK

Email: j.calautit@sheffield.ac.uk

Dr. Ben Richard Hughes

Department of Mechanical Engineering, University of Sheffield, S10 2TN, UK

Email: ben.hughes@sheffield.ac.uk

Abstract

Passive cooling using windcatchers have been utilised in the past by several Middle East countries to capture wind and provide indoor ventilation and comfort without using energy. Recently, researchers have attempted to improve the cooling performance of windcatchers by incorporating heat pipes. The present work encompasses existing research by optimising the arrangement of heat pipes in natural ventilation airstreams using numerical and experimental tools. The airflow and temperature profiles were numerically predicted using Computational Fluid Dynamics (CFD), the findings of which were quantitatively validated using wind tunnel experimentation. Using a source temperature of 314K or 41°C and an inlet velocity of 2.3m/s, the streamwise distance-to-pipe diameter ratio was varied from 1.0 to 2.0 and the emergent cooling capacities were established to comprehend the optimum arrangement. The results of this investigation indicated that the heat pipes operate at their maximum efficiency when the streamwise distance is identical to the diameter of the pipe as this formation allows the incoming airstream to achieve the maximum contact time with the surface of the pipes. In addition, the findings showed that any increase in streamwise spacing leads to the formation of a second bell curve representing an increase in air velocity which simultaneously reduces the contact time between the airstream and the heat pipes, decreasing its effectiveness. The study quantified that the optimum streamwise distance was 20mm at which the S_d/D (streamwise distance-to-pipe diameter) ratio was 1.0. The thermal cooling capacity was subsequently found to decrease by 10.7% from 768W to 686W when the streamwise distance was increased to 40mm (S_d/D ratio of 2.0). The technology presented here is subject to an international patent application (PCT/GB2014/052263).

Keywords: Cooling capacity; heat pipe; streamwise; temperature; wind tunnel

¹Corresponding author

Nomenclature:

A	Cross sectional area (m^2)
ρ	Density of liquid (kg/m^3)
ε	Effectiveness of heat exchanger
g	Gravitational acceleration (m/s^2)
q_{actual}	Heat transfer, actual (W)
q_{max}	Heat transfer, ideal (W)
q_e	Heat transfer rate to evaporator (W)
h_{fg}	Specific enthalpy (J/kg)
c_p	Specific heat capacity of liquid (J/kgK)
ΔT	Temperature difference (K)
$T_{c,inlet}$	Temperature at inlet to condenser (K)
$T_{e,inlet}$	Temperature at inlet to evaporator (K)
$T_{e,outlet}$	Temperature at outlet from evaporator (K)
U	Velocity (m/s)

1. INTRODUCTION

The way in which heat pipes are arranged plays an imperative role on the overall effectiveness of the technology, especially when employed as a passive cooling component in natural ventilation systems. Although a lot of advancements have been made in the field of natural ventilation, they have their own limitations in terms of delivering adequate indoor cooling temperatures largely due to external climatic variations in hot countries. Therefore, the optimisation of passive cooling using energy-efficient heat pipes is of significant interest in the ventilation sector. By incorporating the zero-energy working principles of heat pipes to provide the cooling duty, natural ventilation systems can become an effective and sustainable alternative in keeping the internal environment comfortable [1-3]. In Middle Eastern countries particularly the rapidly developing ones, mechanical air-conditioning is becoming more prevalent and a key contributor to greenhouse gas (GHG) emissions. The extreme conditions of the local climate, inexpensive energy and increased demand for comfort had led to the use of energy-intensive AC in nearly all buildings. This could place buildings at risk of over-heating and not habitable during extremely hot periods. It is crucial for buildings to adapt to such situations without the additional energy-intensive mechanical cooling such as the implementation of passive cooling.

Existing research has indicated the integration of heat pipes into a passive cooling windcatcher to improve its thermal performance [4]. Wind catchers are traditional natural ventilation systems based on the design of traditional architecture, intended to provide ventilation by manipulating pressure differentials around buildings induced by wind movement and temperature difference.

Though the air movement produced by the wind catcher leads to a cooling sensation for occupants, the high air temperature in hot countries often results in lower cooling for occupants. Traditional wind catchers in the past have been integrated with evaporative cooling methods to enhance its cooling performance. However, there are few issues related with the method such as high operation and maintenance cost [23]. Evaporative cooling use a substantial amount of water to run. Hence, this should be taken into consideration in areas where water is expensive or in short supply. In some areas, discarded water from the cooling tower can be an environmental concern. Furthermore, evaporative cooling which

uses wet surface or nozzles requires to be cleaned regularly to avoid mold and bacteria. Other drawbacks associated with the evaporative cooling towers are discussed in [23]. Hence an alternative cooling method for wind catcher is proposed in this work.

Figure 1 displays the cooling operation of a windcatcher with heat pipes inside its channel. The system provides natural ventilation inside a building by capturing warm/hot outdoor air and passing it through the evaporator side of heat pipes which absorbs the thermal energy from the passing airflow and transfer it to a parallel cold sink (condenser). Heat pipes transfer only sensible energy from one airstream to another. Heat pipes do not have moving parts, and failure of the entire unit is infrequent due to minimal risk of corrosion and wear. Space efficiency is another typical characteristic of heat pipes as they can be manufactured in various dimensions depending on the configuration of the energy system. Heat pipes are energy-efficient passive devices and do not consume fossil fuels and other environmentally hazardous resources for carrying out its operation, thereby making itself extremely suitable for use in natural ventilation air streams. There are various heat pipe systems currently available which are applicable to operating temperatures associated with building energy applications [4].

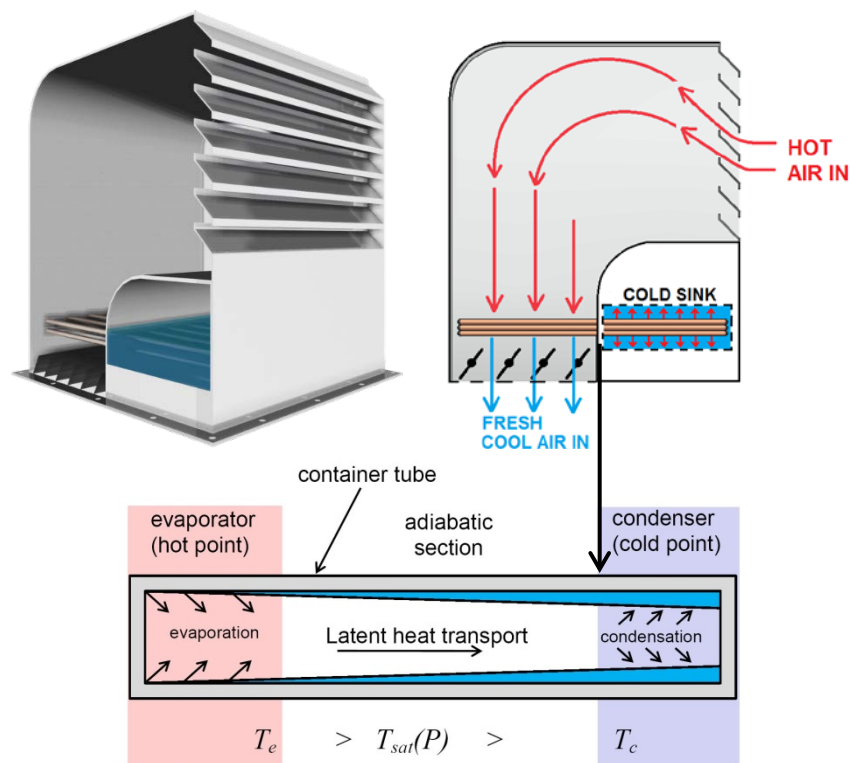


Figure 1 A passive cooling windcatcher with heat pipes to optimise cooling performance [24]

A wide range of studies have been carried out in order to comprehend the thermal behaviour of heat pipes when arranged in a staggered or an inline grid. Generally, staggered arrangements have been found to be more effective than the inline method [5-8]. However, the research on evaluation and optimisation of the cooling capacity of heat pipes in response to varying streamwise configurations are limited in particular its applications in windcatchers. This work therefore investigated the sensible heat transfer and effectiveness of heat pipes in ventilation airstreams by investigating varying streamwise arrangements.

2. PREVIOUS RELATED WORK

Yodrak *et al.*, [9] carried out work on analysing the thermal performance of heat pipes when arranged in both staggered and inline grids. The heat pipe comprised of an evaporator and condenser length of 0.15m along with an adiabatic section of 0.05m. Water was used as the internal working fluid and the internal diameter of the steel heat pipe tube was 0.02m. The arrangement comprised of a total of 8 rows with 6 tubes in each row. Measurements were recorded at the inlet and outlet of the evaporator and condenser section when a steady-state was achieved wherein the temperatures normalised. K-type thermocouples were used as instrumentation for temperature measurement. The mass flow rate of the incoming fluid to the evaporator section was 0.0098 kg/sec. The results of the study established that when the tube arrangement was changed from inline to staggered arrangement, the heat transfer increased from 1,996W to 2,273W. This was primarily due to the staggered arrangement incorporating a larger frontal area of heat pipes than the inline arrangement.

Further to the study carried out by Aris *et al.*, [10] on using fins to enhance heat transfer, the work also investigated the thermal performance of heat pipes arranged under staggered and inline grid structures. The analysis was based on forced convection cooling, thereby indicating the use of heat pipes to carry out the heat duty. The findings indicated that a staggered arrangement of three-dimensional wings as extended surfaces with an aspect ratio of four and an angle of attack of 14° gave the highest enhancement in heat transfer in comparison to the inline arrangement.

Shabgard and Faghri [11] developed a steady-state analytical model for cylindrical heat pipes subjected to a constant heating flux. The proposed model coupled two-dimensional heat conduction in the heat pipe's surface wall along with the liquid flow in the wick and the vapour hydrodynamics. Constant fluid thermophysical properties along with axisymmetric heating and cooling were assumed in the model. The heat pipe was constructed out of copper and distilled water was used as the internal working fluid. The results of the analytical model were compared to full numerical simulations previously conducted by the authors and good correlation was observed. The work found that in certain cases exclusion of the axial heat conduction in the surface wall can cause an error of more than 10% in the calculated pressure drops in heat pipes.

Karthikeyan and Rathnasamy [12] studied the convective heat transfer of pin-fin arrays using the staggered and inline arrangement. The tests were conducted for various mass flow rates of air (Reynolds number ranging from 2,000 to 25,000). The cylindrical cross-section of the pin-fin array included a diameter of 10mm with an overall height of 90mm. A uniform plate heater with a power capacity of 1,500W was used to provide heating temperatures and temperature recordings were undertaken using thermocouples at the inlet and outlet of the evaporator section. The experimental results showed that the staggered pin-fin array significantly enhanced heat transfer as a result of higher turbulence and downstream pressure drop. At a Reynolds number of 4,000, the heat transfer rate using staggered array was approximately

Chaudhry *et al.* [4] compared different heat pipe working fluids in terms of their Merit No. for particular use in building and ventilation systems. Water, ammonia, acetone, pentane and heptane were equated based on their thermophysical fluid properties and the review study revealed that water incorporated the highest Merit No. in relation to other working fluids. At an operating temperature of 293K, the Merit No. for water was 1.78×10^{11} , which was an order higher than ammonia which incorporated a Merit No. of 7.02×10^{10} . In addition, with an increasing operating temperature gradient from 293K to 393K, water

displayed an increase in Merit No. of 64% while other working fluids displayed a reduction in Merit No. as the operating temperatures were increased. As an outcome of the study's findings, water was chosen as the working fluid for the current investigation.

In the author's previous works [1, 22-23], the effect of the heat pipes on the performance of the wind catcher was investigated, highlighting the capabilities of the system to deliver the required fresh air rates and cool the ventilated space. Qualitative and quantitative wind tunnel measurements of the airflow through the wind catcher were compared with the computational modelling and good correlation was observed. Preliminary field testing of the wind catcher was carried out to evaluate its thermal performance under real operating conditions (Figure 2). A cooling potential of up to 12 °C of supply air temperature was identified in this study. Simulation of various external wind speeds (1-5 m/s) showed that the cooling performance of the heat transfer device was indirectly proportional to the air supply rate. At 5 m/s wind speed, the air temperature was only reduced by 5 °C. While, higher temperature reduction was observed at lower wind speed, 9.5 °C reduction at 2 m/s wind speed.



Figure 2 Field testing of passive cooling windcatcher with heat pipe arrangements [23]

This study aims to extend this work by focusing on the heat pipe arrangement optimisation. The work will numerically and experimentally investigate the cooling capacity associated with heat pipes when arranged in a staggered grid with streamwise distance-to-pipe diameter ratios varying between 1.0 and 2.0 at intervals of 0.25. Keeping the geometrical arrangement and external boundary conditions fixed, the flow and thermal profiles of the subsequent airstream was analysed. The rate of heat transfer and effectiveness of the system was determined using both CFD and wind tunnel testing and a correlation between the results was obtained. This work will classify the optimum streamwise arrangement associated with heat pipes for the purpose of passive cooling under ventilation airstreams.

3. COMPUTATIONAL DOMAIN

The computational domain comprised of the purpose-built heat pipe geometry, which was constructed in order to carry out the numerical simulations alongside achieving direct experimental validation. The model was designed according to the specifications of the experimental test section incorporating identical dimensions. 19 cylindrical heat pipes of exact specification were used, which were oriented vertically at an angle of 90° to the ground. The inner and outer diameter of the heat pipes were 0.015m and 0.016m. Figure 3 displays the schematic arrangement of the computational domain.

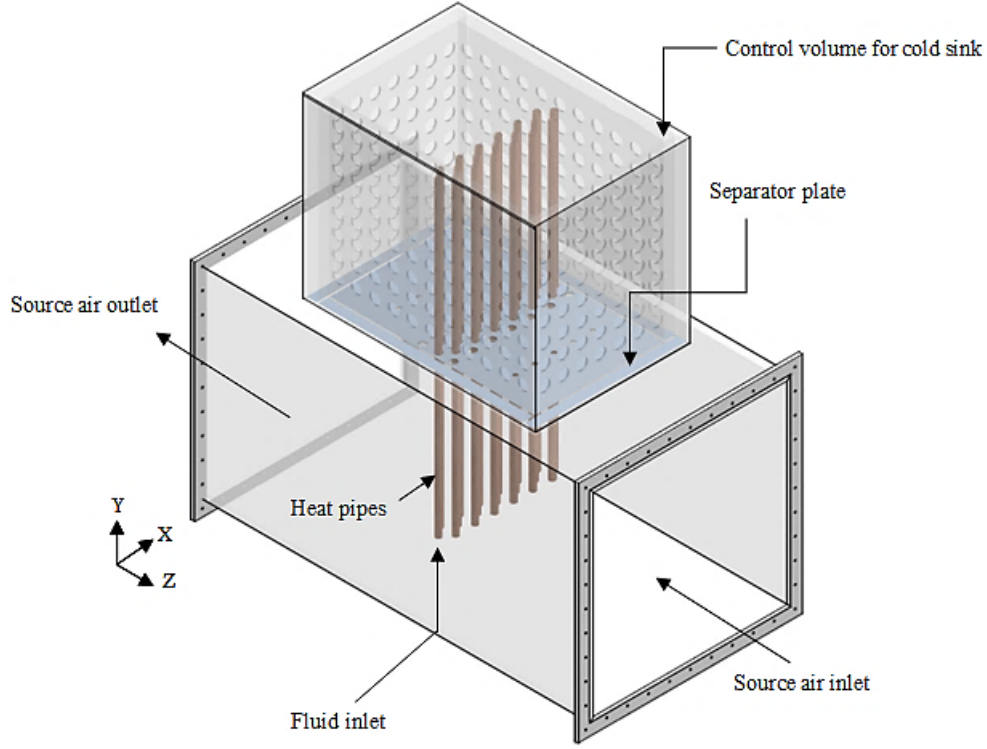


Figure 3 Heat pipe arrangement within the computational domain

The standard k - ϵ transport model which is frequently used for incompressible flows was used to define the turbulence kinetic energy and flow dissipation rate within the model [13, 14]. The use of the standard k - ϵ transport model on cylindrical pipe flows has been found in previous works [15, 16] as has been the approach of integrating Eulerian-Eulerian multiphase simulations alongside [17]. The turbulence kinetic energy, k , and its rate of dissipation, ϵ , are obtained from the following transport equations formulated in eqn.1 and eqn.2.

$$\frac{\partial}{\partial t}(\rho k) + \frac{\partial}{\partial x_i}(\rho k u_i) = \frac{\partial}{\partial x_j} \left[\left(\mu + \frac{\mu_t}{\sigma_k} \right) \frac{\partial k}{\partial x_j} \right] + G_k + G_b - \rho \epsilon - Y_M + S_k \quad (\text{eqn.1})$$

$$\frac{\partial}{\partial t}(\rho \epsilon) + \frac{\partial}{\partial x_i}(\rho \epsilon u_i) = \frac{\partial}{\partial x_j} \left[\left(\mu + \frac{\mu_t}{\sigma_\epsilon} \right) \frac{\partial \epsilon}{\partial x_j} \right] + C_{1\epsilon} \frac{\epsilon}{k} (G_k + C_{3\epsilon} G_b) - C_{2\epsilon} \rho \frac{\epsilon^2}{k} + S_\epsilon \quad (\text{eqn.2})$$

Where; G_k represents the generation of turbulence kinetic energy due to the mean velocity gradients, G_b represents the generation of turbulence kinetic energy due to buoyancy. Y_M represents the contribution of fluctuating dilatation in compressible turbulence to the overall dissipation rate. $C_{1\epsilon}$, $C_{2\epsilon}$ and $C_{3\epsilon}$ are

constants, σ_k and σ_e are the turbulent Prandtl numbers for k and e . S_k and S_e are the user-defined source terms.

The Mixture multiphase model was used to solve the governing equations considering its extensive use in the study of particle transport of two-phase flows through pipes. The Mixture model solves for the mixture momentum equation and prescribes relative velocities to describe the dispersed phases. Accordingly, velocity inlet boundary conditions are applicable to both liquid and vapour phases of the fluid. The SIMPLE algorithm was used for pressure-velocity coupling in order to incorporate the mass transfer terms implicitly into the general matrix and to solve for corrections of pressure and velocity sequentially. Second Order Upwind discretisation scheme was used to obtain the face fluxes for all cells, including those near the interface.

Mass transfer phenomenon for phase interaction between the vapour and liquid species was carried out using the evaporation-condensation mechanism involving the fluid saturation properties. The evaporation-condensation model is a systematic model [18] with a physical basis and solves the mass transfer based on the following temperature regimes as formulated in eqn.3 and eqn.4.

$$\text{If } T > T_{sat} \quad \dot{m}_{e \rightarrow v} = coeff \times \alpha_l \rho_l + \left(\frac{T - T_{sat}}{T_{sat}} \right) \quad (\text{eqn.3})$$

$$\text{If } T < T_{sat} \quad \dot{m}_{e \rightarrow v} = coeff \times \alpha_v \rho_v + \left(\frac{T - T_{sat}}{T_{sat}} \right) \quad (\text{eqn.4})$$

Where; $\dot{m}_{e \rightarrow v}$ represents the rates of mass transfer from the liquid phase to the vapour phase, α and ρ are the phase volume fraction and density.

3.1 Mesh generation

Mesh generation is one of the most important processes in CFD simulation. The quality of the mesh plays a significant role on the accuracy of results and the stability of the solution. A mesh or grid is the representation of the continuous physical surface and volume of an object through a set of discrete x , y , z coordinates.

The meshed model comprised of 160,736 nodes and 778,932 combined tetrahedral and hexahedral elements to obtain a balance between the run time and the resolution in the channel axial direction. The maximum and minimum sizes of the mesh elements were obtained at 7.33×10^{-2} m and 3.66×10^{-4} m while the maximum face sizing was 3.66×10^{-2} m. Higher resolution of mesh was used on the heat pipes (near wall mesh refinement) and in close proximity while lower resolution was used further away from the subject in order to obtain superior precision of results. A total of 7,799 hexahedral elements were applied on the heat pipe tubes with the grid lines perpendicular to the wall surfaces for accurately resolving the viscous and thermal boundary layer. Figure 4 displays the mesh generation on the computational domain.

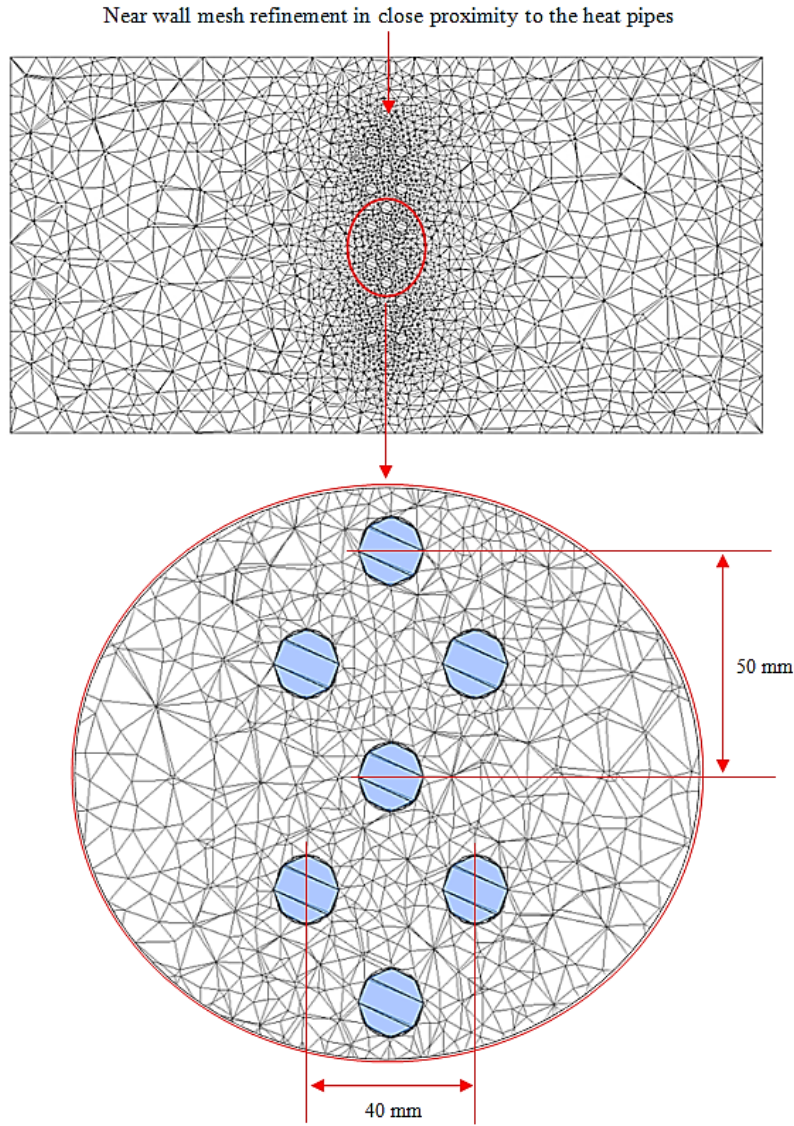


Figure 4 Schematic showing high resolution used in the proximity of the pipes, and lower resolution at a larger distance away from the pipes

The y^+ is a non-dimensional wall distance for a wall-bounded flow commonly used in boundary layer theory and can be defined by eqn.5.

$$y^+ = \frac{u_* y}{\nu} \quad (\text{eqn.5})$$

Where u_* is the friction velocity at the nearest wall, y is the distance to the nearest wall and ν is the kinematic viscosity of the fluid. The critical y^+ values of the grid on the walls of the heat pipe were in the range of 28 and 45, with the average weighted average across the axial length of the heat pipe tubes being 37 remained as per the recommended range which constitutes to $y^+ > 30$ in the entire domain [19, 20].

3.2 Boundary conditions

The applied boundary conditions on the heat pipe heat exchanger computational domain comprised of an initial air velocity of 2.3m/s perpendicular to the hot channel. The cross-sectional area of the test section was 0.25m² thereby indicating a Reynolds number of 62,299 (a mass flow rate of 0.631kg/sec) of air at the evaporator section through convection. A source temperature of 314K was applied to the evaporator section while the condenser section was maintained at 288K. Table 1 indicates the summarised applied boundary conditions applied on the heat pipe heat exchanger.

Table 1 Applied boundary conditions

Parameter	Value / description
Multiphase model	Mixture model
Viscous model	k-epsilon
Near-wall treatment	Enhanced wall functions
Phase 1	Vapour
Phase 2	Liquid
Saturation temperature	293K
Inlet source temperature	314K
Inlet sink temperature	288K
Inlet air velocity	2.3m/s
Velocity formulation	Absolute
Solver type	Pressure based
Gravity	-9.81m/s ² (Y direction)

The control volume of the cold sink located directly above the evaporator section was set to a temperature of 288K and was used as the condenser section of the heat pipes. The temperature in the cold sink was maintained using flexible ice pockets which were positioned at all the four walls of the interface. Each ice pocket had a fill volume of 12ml and a total of 49 ice pockets were used per side of the cold sink. The thermal behaviour of the cold sink was initially monitored without the heat pipes and the stabilised temperature was recorded for 133 minutes corresponding to 2.2 hours. This information was used to determine the length of time for carrying out the experimentation involving heat transfer from heat pipes.

Five computational models were created for the purpose of this investigation with increasing streamwise arrangements between the heat pipes. The spanwise thickness (St) was kept constant at 50mm while the streamwise distance was increased from 20mm to 40mm in 5mm increments (Figure 5). In order to conduct a fair assessment, all boundary conditions were kept identical throughout the thermal analyses.

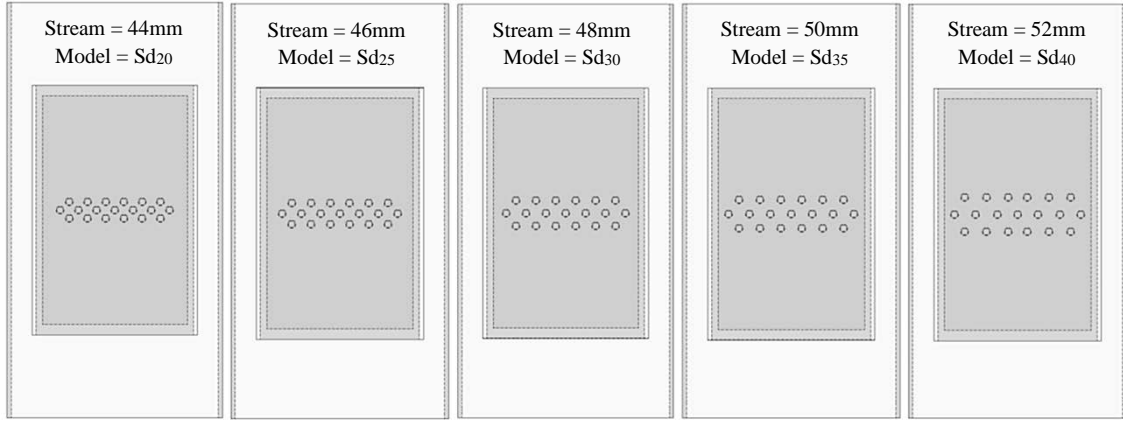


Figure 5 Physical domain illustrating the streamwise distance for the analysed models

Table 2 indicates the ratio of increasing streamwise distances to the diameter of the heat pipe groove. The ratio of Sd/D was increased from 1.0 to 2.0 while the ratio of St/D was kept fixed at 2.5.

Table 2 Streamwise distance models

Model	D (mm)	St (mm)	Sd (mm)	St/D	Sd/D
Sd ₂₀	20.0	50.0	20.0	2.5	1.00
Sd ₂₅	20.0	50.0	25.0	2.5	1.25
Sd ₃₀	20.0	50.0	30.0	2.5	1.50
Sd ₃₅	20.0	50.0	35.0	2.5	1.75
Sd ₄₀	20.0	50.0	40.0	2.5	2.00

4. EXPERIMENTAL SET-UP

The experimental testing was carried out at the University of Leeds Building Physics Laboratory using a low-speed closed-loop wind tunnel to validate the numerical results. The elevation plan of the low-speed closed-loop wind tunnel facility along with the experimental set-up is displayed in Figure 6. The flow in the wind tunnel was characterised prior to experimental testing to indicate the non-uniformity and turbulence intensity in the test-section which was 0.6% and 0.49% and according to the recommended guidelines [21, 22]. The wind tunnel tests were conducted at the same inlet wind speed and temperature as the simulation for the purpose of validation.



Figure 6 Closed-loop wind tunnel showing the experimental set-up for heat pipe testing

The test-section of the wind tunnel was used as the testing rig for carrying out the experimentation while the cold sink was used as the control volume for the condenser section at the top. The set-up comprised of 19 cylindrical heat pipes arranged at 90° vertical to the ground in a staggered grid with a streamwise distance of 20mm (Sd/D ratio of 1.0) and a spanwise thickness of 50mm. The diameter of the copper-water heat pipes was 16mm with a total length of 800mm. The PICO Type K Thermocouple (exposed wire, Polytetrafluoroethylene (PTFE) insulated) with a tip diameter of 1.5mm and a tip temperature range between -75°C to 250°C was used for the experiment.

The boundary layer thickness of the test-section was 0.05m and the heat pipes were located outside the boundary layer region for accurate evaluation. Discrete points (Figure 7) were located at the inlet and outlet of the physical domain in order to quantify the performance of the heat pipe system at specific measurement locations. The origin was the base of the test section directly underneath the central heat pipe. The thermocouple points were located 0.15m upstream (I_1 and I_2) and downstream ($O_1 - O_5$) of the heat pipe physical domain (Z-direction), spaced 0.05m apart in the X-direction. The Y-direction was kept constant at 0.25m.

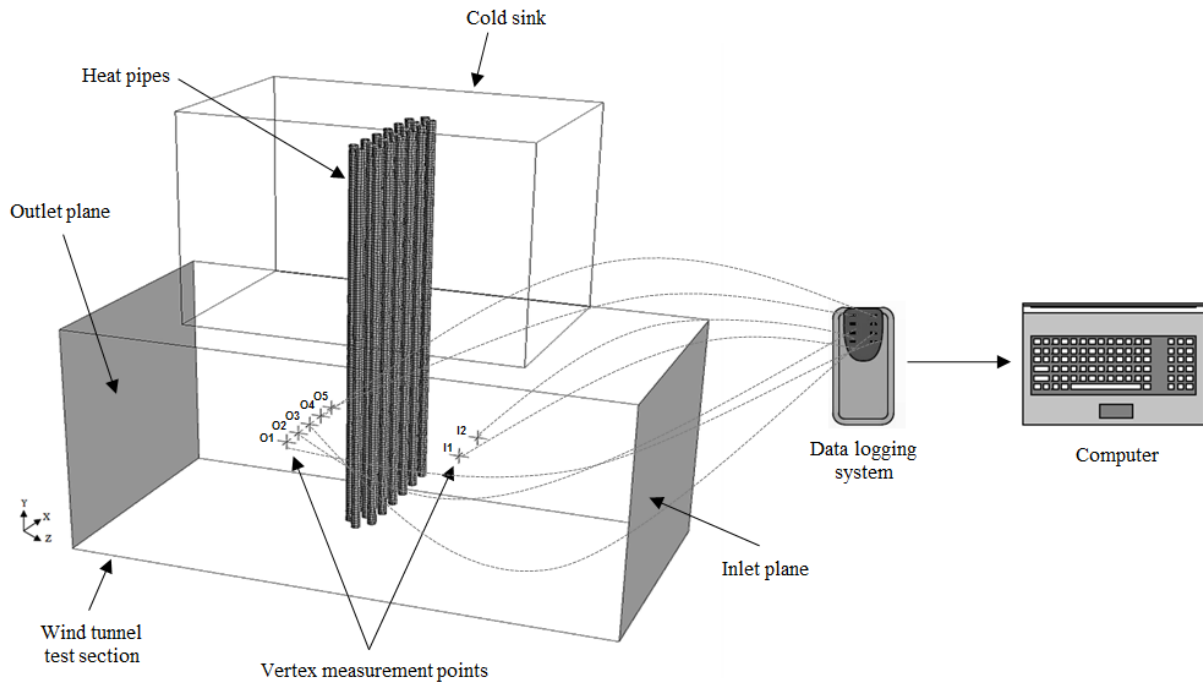


Figure 7 Measurement point locations at the inlet and outlet of the physical domain

4.1. Heat pipe specification

Heat pipes in the past have been integrated into the heat exchanger systems in buildings for the purpose of pre-heating fresh air. However, their potential to operate in reverse to deliver passive cooling is now gaining momentum. For this study, cylindrical copper heat pipes were manufactured as per the design specifications. The dimensions of the evaporator and condenser sections and the main parameters of the manufactured heat pipes are displayed in Figure 8.

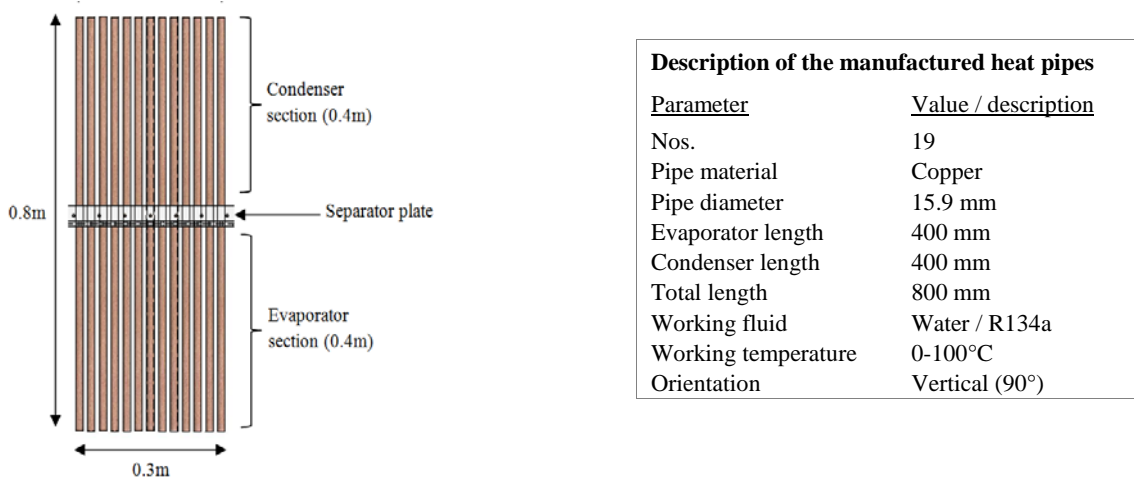


Figure 8 Main parameters of the manufactured heat pipes

The heat pipes were charged with water and R-134a as the working fluids comprising of 2/3rd of the evaporator length, thus indicating a fluid volume of 0.000054m³. The working sub-atmospheric pressures were set to saturation and at an operating temperature of 293K. The heat pipes were vacuum sealed at the end of the tube with the end cap incorporating a diameter of 3mm greater than the actual pipe diameter. The total length of the heat pipes was 800mm and the sections were separated in the centre using a connecting plate allowing identical evaporator and condenser sectional lengths of 400mm each.

4.2. Data reduction

A precise experimental determination of the thermal performance of the heat pipe heat exchanger requires accurate measurement of the temperatures of the air flow at different locations of the heat exchanger, to determine the rate of heat transfer across the length of the heat exchanger. Characterisation of the evaporator section was carried out by averaging the temperature measurements at the respective locations at regular intervals of time. Air density and specific heat capacity values were taken in accordance with the source temperatures. The rate of heat transfer at the evaporator section (test-section of the wind tunnel) is formulated using eqn.6.

$$q_e = \rho_G U A C_{p,G} (T_{e,inlet} - T_{e,outlet}) \quad (\text{eqn.6})$$

Quantification of the thermal performance of heat pipes is based on the concept of heat exchanger effectiveness. The effectiveness of a heat exchanger is the ratio of actual rate of heat transfer by the heat exchanger to the maximum possible heat transfer rate between the air as formulated in eqn.7.

$$\varepsilon = \frac{q_{actual}}{q_{max}} = \frac{T_{e,inlet} - T_{e,outlet}}{T_{e,inlet} - T_{c,inlet}} \quad (\text{eqn.7})$$

5. RESULTS AND DISCUSSION

5.1. Flow and thermal profiles

The computational investigation predicted the air velocity, pressure and temperature profiles upstream and downstream of the heat pipes within the test section. Based on the evaluation of the highest temperature reduction, the optimum heat pipe configuration in terms of streamwise distance was determined. Figure 9 displays the air velocity streamlines along with air pressure and temperature contour levels for each of the analysed models.

Figure 9 (a) displays the air velocity streamlines and due to the streamlined cross-section of the cylindrical tubes, a similar velocity trend to varying spanwise thickness models was obtained once again. The inlet velocity was kept constant at 2.3m/s for all cases and the findings showed that the velocity increased by approximately 0.9m/s at both ends of the bank of the tubes. A decrease in air velocity was noted at the immediate downstream of the heat pipes due to the contact period between the fluid and the pipe surface. With respect to Figure 9 (b), the static pressure contours for all models are highlighted. Positive pressure regions were created at the upstream of the rows of heat pipes for all analysed models with a mean value of 4.1Pa. Correspondingly, the downstream locations of the heat pipes experienced a region of negative pressures with a mean value of -0.3Pa noted across all models.

Temperature contour levels are illustrated in Figure 9 (c). The temperature of air decreased as the stream passed over the pipes due to the transfer of heat between the air stream and the heat pipes. Maximum temperature reduction was noted at the immediate downstream locations of the heat pipes where the air velocity was the lowest indicating a direct proportionality between the two quantities. Simultaneously, there was no temperature reduction on either side of the bank of the pipes since there was no contact between the airstream and the heat pipes.

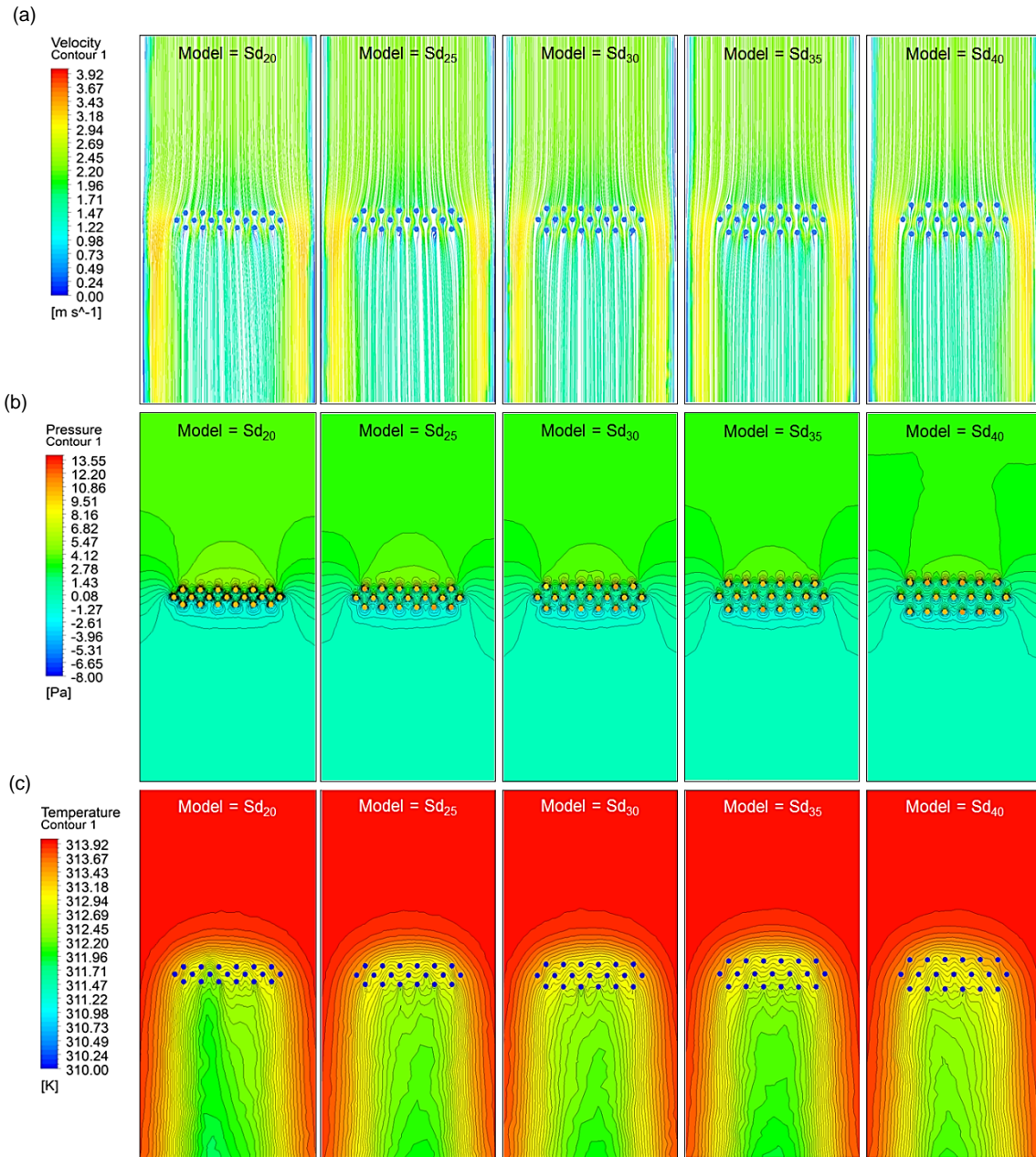


Figure 9 Contour levels displaying air: (a) velocity (b) pressure (c) temperature for the analysed streamwise distance models

For Sd₂₀ (streamwise distance = 20mm) model, the variation in air temperature and velocity across the axial length of the test section is displayed in Figure 10. At an inlet velocity of 2.3m/s, the maximum velocity value was determined at 2.55m/s as the airstream came in contact with the 1st row of heat

pipes. Overall, the air velocity was reduced by 45.3%. With respect to the airside axial thermal profile, the Sd_{20} model displayed the optimum results in terms of temperature reduction as a minimum temperature value of 311.8K was estimated, highlighting a temperature drop of 2.2K or 0.67%.

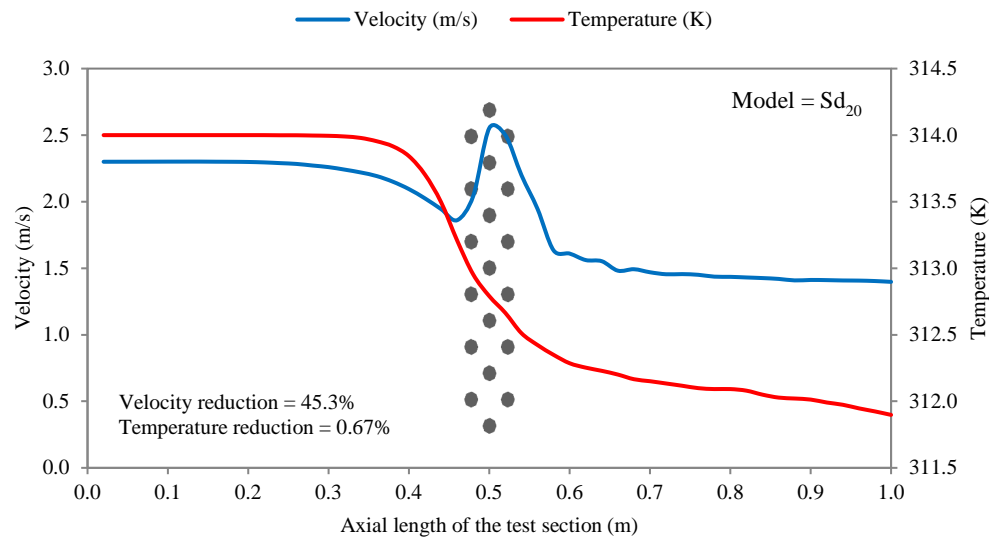


Figure 10 Variation in air velocity and temperature profile before and after contact with heat pipes for Sd_{20} model

Figure 11 displays the quantification of air velocity and temperature results for the Sd_{25} (streamwise distance = 25mm) model. The trend in velocity profile was dissimilar to the Sd_{20} model with a maximum velocity value of 2.43m/s obtained prior to the 1st row of heat pipes. As the Sd/D (streamwise distance-to-pipe diameter) ratio increased above unit to 1.25, the formation of the second velocity peak became evident, thereby indicating a reduction in contact time between the air stream and the heat pipes. The minimum velocity value was estimated at 1.43m/s as the airstream came in contact with the three rows of heat pipes. Inlet temperature was set to 314K and a reduction percentage of 0.63% was noted for the Sd_{25} streamwise distance model in comparison to 0.67% for the Sd_{20} model.

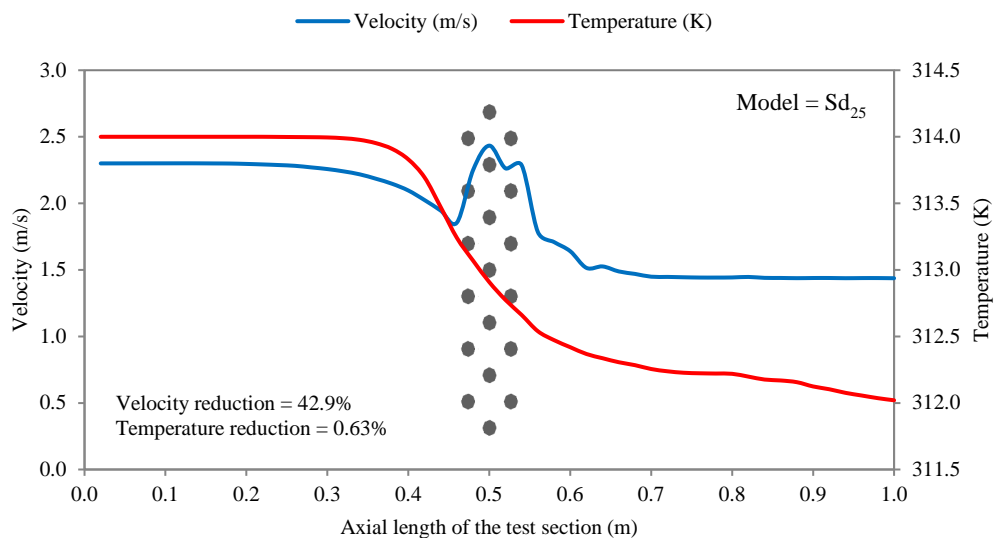


Figure 11 Variation in air velocity and temperature profile before and after contact with heat pipes for Sd₂₅ model

Figure 12 shows the air velocity and temperature trend for the Sd₃₀ (streamwise distance = 30mm) model. Like the Sd₂₅ model, two distinct velocity peak points were observed as the streamwise distance between rows was increased to 30mm. This effect was predominantly due to the increasing distances between the individual rows, providing time for the airstream to reach regions of high velocities on two instances. The maximum air velocity was determined at 2.54m/s while the mean air velocity was 1.91m/s. The temperature profile continued to indicate a lower reduction in air temperature with increasing streamwise distances as a reduction 1.96K or 0.62% was calculated.

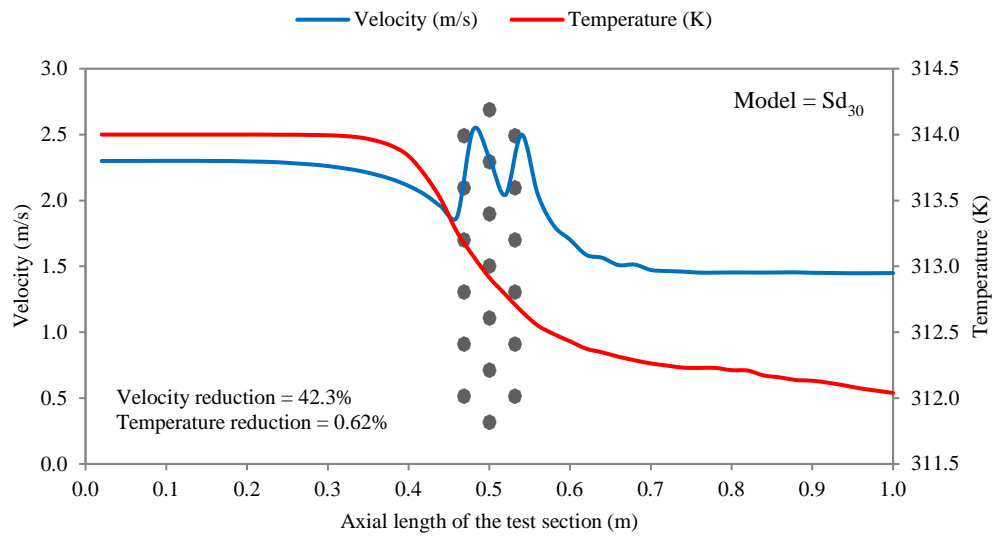


Figure 12 Variation in air velocity and temperature profile before and after contact with heat pipes for Sd₃₀ model

The streamwise distance was further increased to 35mm and the quantified air velocity and temperature results for Sd₃₅ (streamwise distance = 35mm) model are displayed in Figure 13. The formation of two velocity peaks was evident at the start of the 1st and 3rd row of heat pipes. The highest velocity was noted at 2.51m/s which was 0.02m/s lower than the Sd₃₀ model. The velocity was found to decrease to a minimum value of 1.45m/s downstream of the heat pipes. The air temperature decreased from the inlet value of 314K to approximately 312K after contact with the heat pipes. The temperature profile obtained from the Sd₃₅ model was very similar to the Sd₃₀ model as a reduction percentage of 0.61% was calculated.

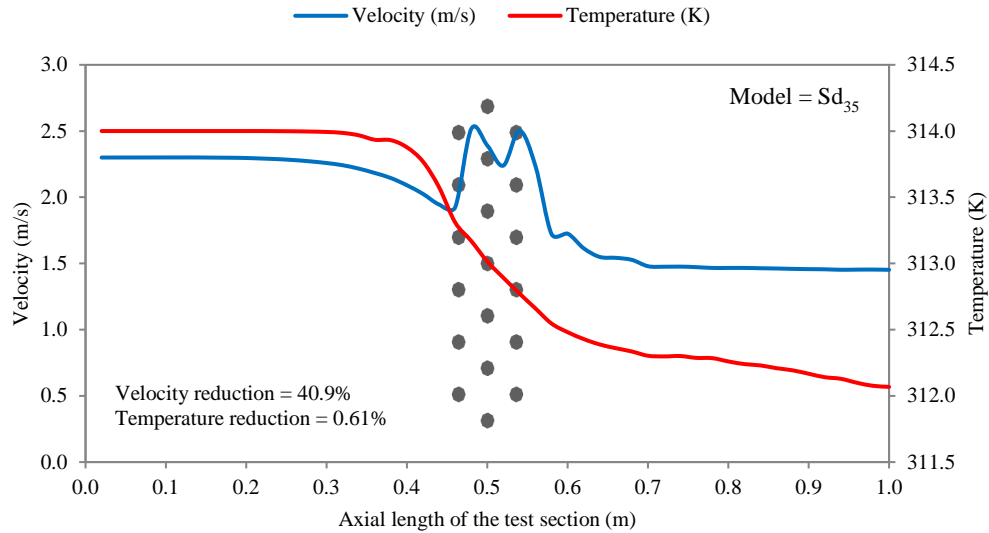


Figure 13 Variation in air velocity and temperature profile before and after contact with heat pipes for Sd₃₅ model

The maximum streamwise distance analysed from the current geometry was 40mm or twice the pipe diameter. Figure 14 displays the findings obtained from the Sd₄₀ (streamwise distance = 40mm) model. A maximum velocity value of 2.46m/s was noted at the upstream of the 1st row of heat pipes. This arrangement provided the lowest reduction in air velocity as a reduction percentage of only 40% was obtained. This was due to the increased spacing between the rows of the heat pipes with the Sd/D (streamwise distance-to-pipe diameter) ratio of 2.0. With respect to the thermal profile, the Sd₄₀ model indicated the lowest reduction in air temperatures, calculated at only 1.83K or 0.58%. From all analysed models it was concluded that the Sd₂₀ model provided the greatest reduction in air temperatures across the axial length of the test section.

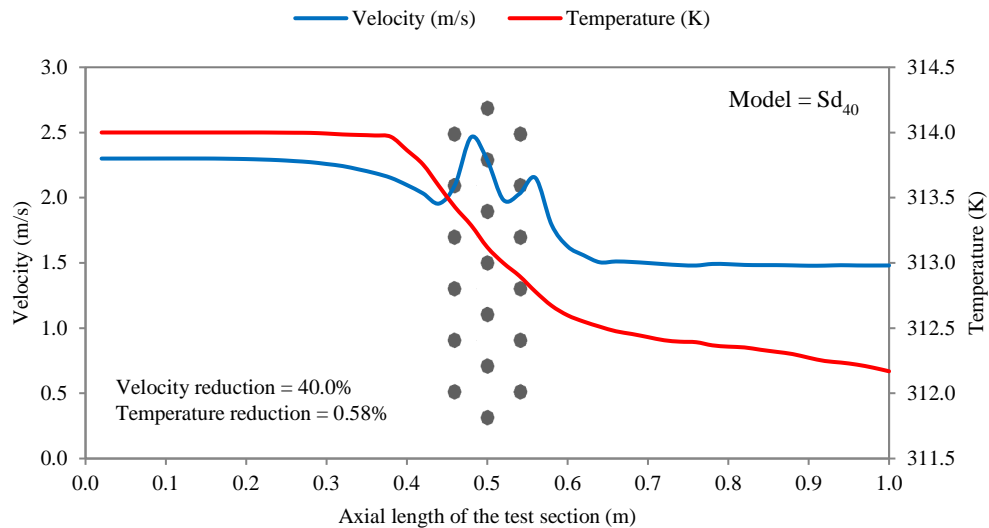


Figure 14 Variation in air velocity and temperature profile before and after contact with heat pipes for Sd₄₀ model

Table 3 summarises the mean values of the air velocity and temperature for all streamwise distance models at the measurement locations. Keeping a constant inlet air temperature of 314K for all cases, maximum temperature difference (ΔT) was obtained for the Sd₂₀ model at 1.68K. In general, the temperature differentials decreased as the streamwise distance increased with the lowest ΔT calculated for the Sd₄₀ model at 1.55K. An inverse proportionality was thus established between the decreasing temperature reductions and the increasing streamwise distances between the rows of heat pipes.

Table 3 Summary of the mean parametric values obtained for streamwise distance models

Model	Mean inlet velocity (m/s)	Mean outlet velocity (m/s)	Δv (m/s)	Mean inlet temperature (K)	Mean outlet temperature (K)	ΔT (K)
Sd ₂₀	2.20	1.46	0.84	313.96	312.32	1.68
Sd ₂₅	2.20	1.50	0.80	313.96	312.33	1.67
Sd ₃₀	2.19	1.50	0.80	313.97	312.42	1.58
Sd ₃₅	2.19	1.51	0.79	313.97	312.43	1.57
Sd ₄₀	2.19	1.55	0.75	313.97	312.45	1.55

In addition, the analysis determined that the mean outlet velocity increased from 1.46m/s to 1.55m/s as the streamwise distance was increased from 20mm to 40mm. The maximum reduction in air velocity (Δv) was calculate for the Sd₂₀ model at 0.84m/s while the minimum reduction in air velocity was depicted at 0.75m/s for the Sd₄₀ model. The bar graph representation of the parametric reductions in air velocity and temperature for all analysed streamwise distance models are displayed in Figure 15.

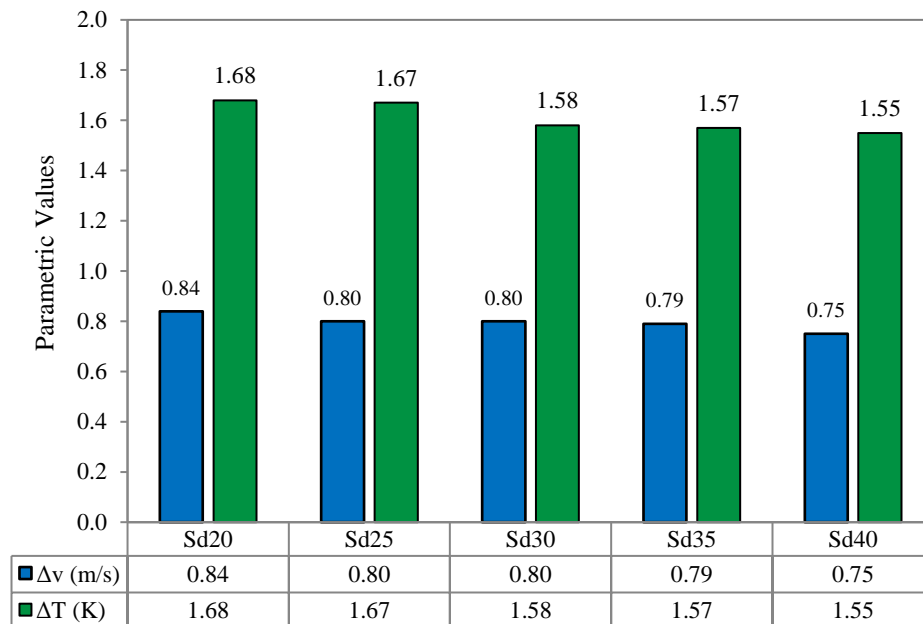


Figure 15 Bar chart representation of the difference in air velocity and temperature for streamwise distance models

5.2. Total cooling capacity and overall effectiveness

Similar to the spanwise arrangement models, the area-weighted averaged cooling capacity or heat transfer, upstream and downstream of the heat pipes was further evaluated. This section established the quantified results for the cooling capacity (rate of heat transfer) and effectiveness obtained from the analysis of all five streamwise distance models. The summarised findings for heat transfer and overall heat pipe effectiveness are displayed in Table 4. The highest mean overall effectiveness was calculated at 5.6% for the Sd₂₀ model while the lowest mean overall effectiveness was calculated at 5.0% for the Sd₄₀ model. The highest rate of heat transfer in the test section was 768.17W for the Sd₂₀ model. A variation of 82.3W was achieved between the highest and lowest rate of heat transfer from the compared models.

Table 4 Summary of the mean heat transfer values obtained for streamwise distance models

Model	Evaporator net heat transfer (W)	Overall effectiveness (%)
Sd ₂₀	768.17	5.60%
Sd ₂₅	764.25	5.57%
Sd ₃₀	705.46	5.14%
Sd ₃₅	698.93	5.10%
Sd ₄₀	685.87	5.00%

The graphical representation of the cooling capacity and heat pipe effectiveness results are plotted Figure 16. The total cooling capacity or heat transfer was directly proportional to the overall effectiveness of the heat pipe system since all other parameters apart from air temperature were kept constant throughout the investigation. Since the temperature differential reduced as the streamwise distances increased from 20mm (Model Sd₂₀) to 400mm (Model Sd₄₀), a decreasing gradient was observed for both total heat transfer rate and overall effectiveness of the heat pipe heat exchanger.

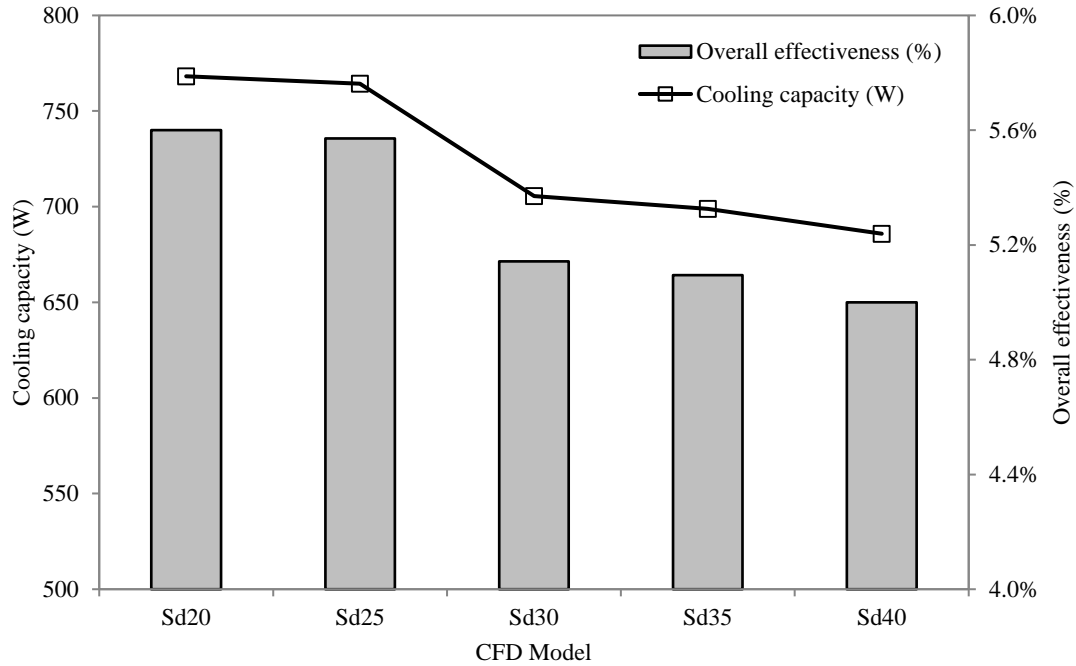


Figure 16 Relationship between cooling capacity and overall heat exchanger effectiveness for streamwise distance models

In summary, the results of this investigation indicated that the heat pipes operate at their maximum efficiency when the streamwise distance is identical to the diameter of the pipe as this formation allows the incoming airstream to achieve the maximum contact time with the surface of the pipes. The study showed that any increase in streamwise spacing leads to the formation of another bell curve representing an increase in air velocity which simultaneously reduces the contact time between the airstream and the heat pipes, decreasing its effectiveness. The findings from this study quantified that the optimum streamwise distance was 20mm at which the Sd/D (streamwise distance-to-pipe diameter) ratio was 1.0. The thermal cooling capacity was found to decrease by 10.7% from 768W to 686W when the streamwise distance was increased to 40mm (Sd/D ratio of 2.0). These are important findings indicating the ideal arrangement for heat pipes to be arrayed, to work at their optimum capacity for the purpose of passive cooling in buildings.

5.3. Experimental validation

The experimental validation was carried out on the Sd_{20} model to determine the accuracy of the numerical findings. The test-section of the wind tunnel was used as the control domain and the experimental test incorporated identical boundary conditions as the CFD model. The testing was conducted after allowing the temperature in the test-section to stabilise to the required set-point. At a source temperature of 314K or 41°C, a mean reduction of 1.35°C (Figure 17 a) across was obtained using the experimental run-time of 200 seconds. Figure 17 (b) displays the formation of downstream temperatures when the source temperature was normalised to 41°C or 314K. The downstream temperature formations indicated the actual thermal cooling capacity of heat pipes in response to the source temperature. A highest temperature reduction of 1.6K was obtained during the transient test, indicating a cooling capacity of 1,045W and a heat pipe effectiveness of 6.15%.

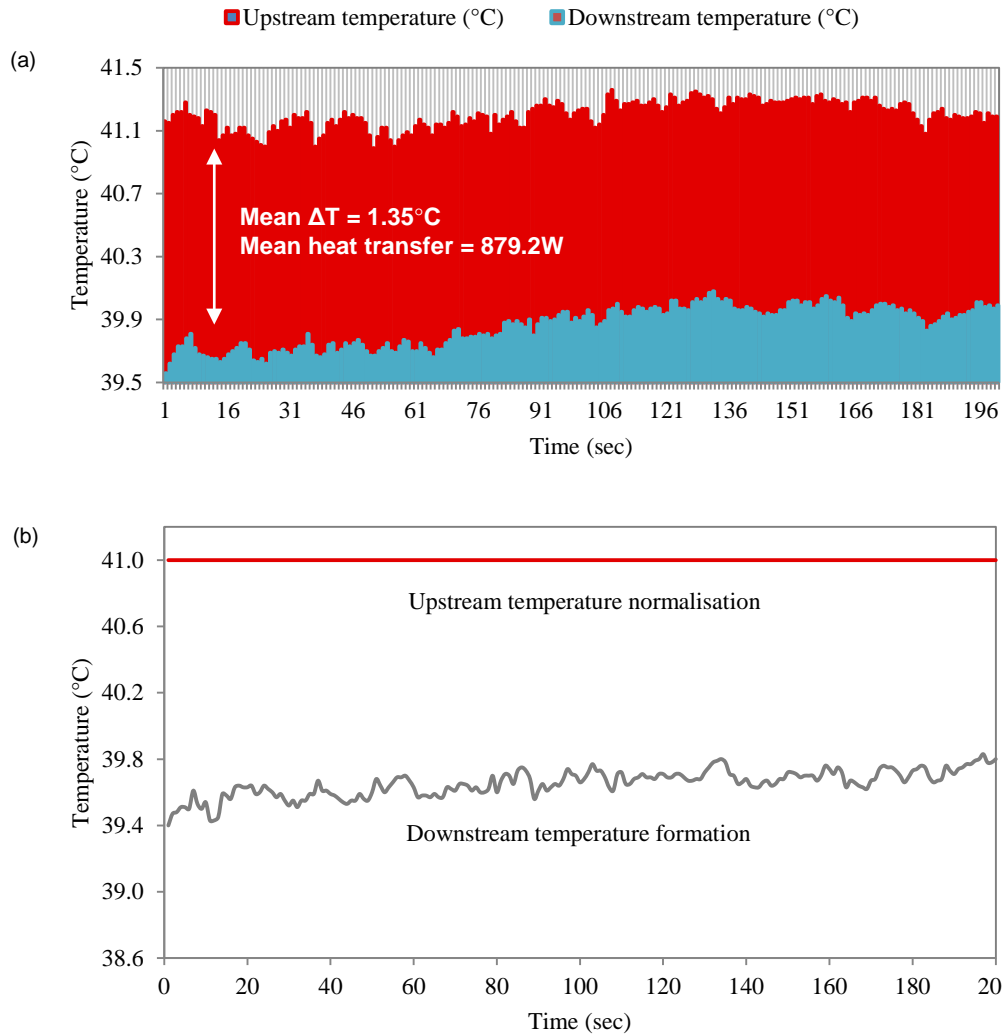


Figure 17 Upstream and downstream air temperatures formation shown in: (a) actual (b) normalised recordings

A quantitative validation of the CFD results was done by recording temperature, velocity and pressure measurements at the discrete measurement point locations and comparing it against the experimentally obtained values. The error percentage at each measuring location for the Sd_{20} model is tabulated in Table 5. A good correlation was observed in temperature results were obtained for this model with a maximum differential of only 1.63%. Measurement location I_1 indicated the highest variation in air velocity and pressure readings with the CFD values overestimating the experimental results by 14.6% and 16.4%. In addition, a good agreement was obtained for air velocity between the two methodologies at the downstream locations with a mean error percentage of 6.4%.

473

Table 5 Error percentage between CFD and experimental results for Sd₂₀ model

Point	CFD (°C)	Exp. (°C)	Error	CFD (m/s)	Exp. (m/s)	Error	CFD (Pa)	Exp. (Pa)	Error
I ₁	40.97	40.95	0.05%	2.19	1.87	14.6%	3.11	2.60	16.4%
I ₂	40.96	40.98	0.05%	2.20	1.88	14.5%	3.09	2.70	12.6%
O ₁	39.31	39.60	0.74%	1.46	1.37	6.2%	1.38	1.50	8.0%
O ₂	39.02	39.40	0.97%	1.44	1.25	13.2%	1.39	1.30	6.9%
O ₃	39.32	39.71	0.99%	1.48	1.42	4.1%	1.50	1.60	6.3%
O ₄	39.38	40.02	1.63%	1.50	1.51	0.7%	1.41	1.20	14.9%
O ₅	39.59	40.23	1.62%	1.42	1.54	7.8%	1.25	1.30	3.8%

474

475

6. CONCLUSION

476

477

478

479

480

481

482

483

484

485

486

487

488

A detailed investigation was carried out into highlighting the optimum heat pipe streamwise spacing for passive cooling of high-temperature ventilation airstreams. The set-up comprised of 19 cylindrical copper-water heat pipes arranged in a staggered grid, 90° with respect to the ground. The cooling capacity or thermal performance of the heat pipes was analysed using varying streamwise distance to diameter ratios ranging from 1.0 to 2.0. The findings of this study determined that the optimum streamwise distance was 20mm at which the Sd/D (streamwise distance-to-pipe diameter) ratio was 1.0. The cooling capacity and system effectiveness was found to decrease by 10.7% from 768W to 686W when the streamwise distance was increased to 40mm (Sd/D ratio of 2.0). Wind tunnel experimental testing was conducted to validate the numerical model at designated point locations. A good agreement was obtained between the numerical and experimental findings with a maximum error of 1.6% for temperature and 14.6% for velocity parameters. The investigation successfully evaluated the performance of heat pipes under varying geometrical arrangement, when utilised for the purpose of pre-cooling convection airstreams, and which can be applied within windcatchers.

489

ACKNOWLEDGEMENT

490

491

492

The research and wind tunnel experimental support provided by the University Of Leeds and Qatar National Research Fund (NPRP09-138-2-059) is gratefully acknowledged by the author. The technology presented here is subject to an international patent application (PCT/GB2014/052263).

493

REFERENCES

494

495

496

497

498

499

500

501

502

503

504

505

1. Hughes BR, Chaudhry HN and Ghani SA, (2011). *A review of sustainable cooling technologies in buildings*, *Renewable and Sustainable Energy Reviews* 15, 3112-3120
2. Arango BS, Hughes BR and Chaudhry HN, (2012). *Performance investigation of ground cooling for the airbus A380 in the United Arab Emirates*, *Applied Thermal Engineering* 36, 87-95
3. Chaudhry HN and Hughes BR, (2011). *Computational analysis of dynamic architecture*, *Journal of Power and Energy*, *Proceedings of the Institution of Mechanical Engineers Part A* 225, 85-95
4. Chaudhry HN, Hughes BR and Ghani SA, (2012). *A review of heat pipe systems for heat recovery and renewable energy applications*, *Renewable and Sustainable Energy Reviews* 16, 2249-2259
5. Van Fossen G, 1981. *Heat transfer coefficients for staggered arrays of short pin fins*, NASA STI/Recon Technical Report No. 81
6. Metzger D, Fan C and Haley S, 1984. *Effects of pin shape and array orientation on heat transfer and pressure loss in pin fin arrays*, *Journal of Engineering for Power* 106(1) 252-257

7. Chyu M, Hsing Y and Natarajan V, 1998. *Convective heat transfer of cubic fin arrays in a narrow channel*, ASME J. Turbomach 120 362-367
8. Rallabandi AP, Liu YH and Han JC, 2011. *Heat transfer in trailing edge wedge shaped pin fin channels with slot ejection under high rotation numbers*, Journal of Thermal Science and Engineering Applications, 3 021007-1-9
9. Yodrak L, Rittidech S, Poomsa-ad N and Meena P, 2010. *Waste Heat Recovery by Heat Pipe Air-Preheater to Energy Thrift from the Furnace in a Hot Forging Process*, American Journal of Applied Sciences 7, 675-681
10. Aris MS, McGlen R, Owen I and Sutcliffe CJ, 2011. *An experimental investigation into the deployment of 3-D finned wing and shape memory alloy vortex generators in a forced air convection heat pipe fin stack*, Applied Thermal Engineering 31, 2230-2240
11. Shabgard H, Faghri A, 2011. *Performance characteristics of cylindrical heat pipes with multiple heat sources*, Applied Thermal Engineering 31, 3410-3419
12. Karthikeyan R, Rathnasamy R, 2011. *Thermal performance of pin-fin arrays*, International Journal of Advanced Engineering Sciences and Technologies 10, 125-138
13. Launder BE and Spalding DB, 1972. *Lectures in mathematical models of turbulence*, Academic Press, London, England
14. Chung TJ, (2002). *Computational Fluid Dynamics*, Cambridge University Press; illustrated edition edition, ISBN-0521594162
15. Ekambara K, Dhotre MT, Joshi JB, (2006). *CFD simulation of homogeneous reactions in turbulent pipe flows-Tubular non-catalytic reactors*, Chemical Engineering Journal 117, 23-29
16. Saber MH, Ashtiani HM, (2010). *Simulation and CFD Analysis of heat pipe heat exchanger using Fluent to increase of the thermal efficiency*, Proceedings of the 7th WSEAS International Conference on Heat and Mass Transfer, Cambridge
17. Ekambara K, Sanders RS, Nandakumar K, Masliyah JH, (2008). *CFD simulation of bubbly two-phase flow in horizontal pipes*, Chemical Engineering Journal 144, 277-288
18. Lee WH, (1979). *A Pressure Iteration Scheme for Two-Phase Modeling*, Technical Report LA-UR 79-975, Los Alamos Scientific Laboratory, Los Alamos, New Mexico
19. ANSYS Fluent User's Guide, (2011). ANSYS, Inc. Southpointe November 2011, 275 Technology Drive, Canonsburg, PA 15317 Release 14.0
20. Versteeg HK and Malalasekera V, (2007). *An Introduction to Computational Fluid Dynamics: The Finite Volume Method*, Second Edition, Pearson Education Limited 1995, 2007
21. Calautit JK, Chaudhry HN, Hughes BR and Sim, LF, (2014). *A validated design methodology for a closed-loop subsonic wind tunnel*, Journal of Wind Engineering and Industrial Aerodynamics 125, 180-194
22. Chaudhry HN and Hughes BR, (2014). *Analysis of the thermal cooling capacity of heat pipes under a low Reynolds number flow*, Applied Thermal Engineering 71, 559-572
23. Calautit JK and Hughes BR (2016). *A passive cooling wind catcher with heat pipe technology: CFD, wind tunnel and field-test analysis*, Applied Energy, 162, 15, 460-471
24. Calautit JK, Hughes BR & Sofotasiou P (2016) *Design and Optimisation of a Novel Passive Cooling Wind Tower*, 14th International Conference on Sustainable Energy Technologies SET 2015 - 25th to 27th August 2015, Nottingham UK